JOURNAL OF GEOPHYSICAL RESEARCH, VOL. 100, NO. E1, PAGES 1553–1563, JANUARY 25, 1995

Volatile transport on Venus and implications for surface geochemistry and geology

Robert A. Brackett, Bruce Fegley Jr., and Raymond E. Arvidson

Department of Earth and Planetary Sciences and McDonnell Center for the Space Sciences, Washington University St. Louis, Missouri

Abstract. The high vapor pressure of volatile metal halides and chalcogenides (e.g., of Cu, Zn, Sn, Pb, As, Sb, Bi) at typical Venus surface temperatures, coupled with the altitude-dependent temperature gradient of ~8.5 K km^{-1}, is calculated to transport volatile metal vapors to the highlands of Venus, where condensation and accumulation will occur. The predicted geochemistry of volatile metals on Venus is supported by observations of Cu, Zn, Sn, Pb, As, Sb, and Bi minerals around terrestrial volcanic vents, spectroscopic observations of CuCl in volcanic gases at Kilauea and Nyiragongo, and large enrichments of these and other volatile elements in terrestrial volcanic aerosols. A one-dimensional finite difference vapor transport model shows the diffusive migration of a thickness of 0.01 to >10 μm/yr of moderately to highly volatile phases (e.g., metal halides and chalcogenides) from the hot lowlands (740 K) to the cold highlands (660 K) on Venus. The diffusive transport of volatile phases on Venus may explain the observed low emissivity of the Venusian highlands, hazes at 6-km altitude observed by two Pioneer Venus entry probes, and the Pioneer Venus entry probe anomalies at 12.5 km.

Introduction

The mean horizontally polarized microwave emissivity of Venus is 0.85 as determined from Magellan 12.6 cm data [*Pettengill et al.*, 1992]. This emissivity is expected from a surface composed of bedrock and/or well-consolidated soil. However, at high elevations (≥6055 km radius) emissivities range from ~0.3 to ~0.9 and mean emissivities decrease to values as low as 0.4. Such low emissivities are not explainable in terms of simple rock or soil surfaces, and therefore a unique mechanism (chemical, textural, etc.) must be invoked. Various models have been proposed to explain the low emissivity of the highlands of Venus including the presence of pyrite [*Pettengill et al.*, 1982, 1988], perovskite [*Fegley et al.*, 1992], ferroelectrics [*Shepard et al.*, 1994], decimeter-scale voids [*Pettengill and Ford*, 1993], or a low-loss soil layer [*Tryka and Muhleman*, 1992]. Problems exist with each of these models. Pyrite is unlikely to be responsible, as it is thermodynamically unstable and is rapidly destroyed on a geologic timescale [*Fegley and Treiman*, 1992; *Fegley et al.*, 1993; *Klingelhöfer et al.*, 1994]. Perovskite has a high dielectric constant, $\varepsilon \sim 170$, but abundances of >20% are required to account for observed highland emissivities. Ferroelectrics reproduce observed highland emissivities [*Shepard et al.*, 1994], but a specific mineral phase has not been identified. Microwave scattering from decimeter-scale voids or a low-loss soil layer are possible, but no geologic mechanism has been put forward. Here, we investigate the effects of vapor transport of volatile phases and discuss implications for microwave signatures, surface geochemistry and weathering, and the near-surface atmosphere of Venus.

Copyright 1995 by the American Geophysical Union.

Paper number 94JE02708.
0148-0227/95/94JE02708$05.00

At the global mean temperature of Venus, $T \sim 740$ K, vapor pressures of nearly all metal halides and chalcogenides are 10^{20} times greater than on the Earth ($T \sim 288$ K) [*Knacke et al.*, 1991]. From 0- to 10-km elevation, vapor pressures of metal halides and chalcogenides drop by 1–3 orders of magnitude. The net effect of high vapor pressures and strong concentration gradients is that the Venusian highlands act as "cold traps" for volatile vapors [*Fegley*, 1993]. *Lewis* [1968] first proposed the concept of volatile transport on Venus. Operating on the assumption of a large latitudinal temperature gradient, Lewis proposed that volatile transport may occur towards polar regions. However, it is now known that the maximum temperature range with altitude is >80 K whereas the maximum temperature range with latitude is probably ~10-20 K [*Kuz'min*, 1983; *Seiff*, 1983].

Several other studies have considered volatile element geochemistry on Venus with an emphasis on explaining the chemistry of the global clouds. *Lewis* [1969] examined the possibility of mercury halides (and selected other halides and sulfides) existing in the visible cloud deck on Venus (40+ km altitude). *Barsukov et al.* [1981] also investigated possible cloud-forming volatiles including a number of metal (e.g., Ag, Bi, Cd, Cu, Pb, Zn) halides and sulfides. Claims of detection of chlorine condensates in the main cloud deck from Venera 11/12 and Vega 1/2 experiments have been made [*Surkov et al.*, 1981, 1982, 1987; *Petryanov et al.*, 1981; *Andreichikov et al.*, 1987], but the geochemical plausibility of these observations has been questioned [*Lewis and Fegley*, 1982; *Fegley and Treiman*, 1992]. Here, we examine the role of metal halides and chalcogenides at the surface and in the lower atmosphere (<15 km) of Venus.

Terrestrial Volcanic Gases and Sublimates

We focus on metal halides and chalcogenides because they are commonly observed in terrestrial volcanic gases, condensates, and sublimates (see Table 1). Chalcophilic and volatile elements in volcanic gases are enriched by up to 8 orders of magnitude relative to associated basalts for ocean island basaltic volcanism and arc volcanism (see Table 2).

Table 1. Minerals Found Near Terrestrial Volcanic Vents or Fumaroles

Mineral Name	Chemical Formula	References
Acmite	$NaFeSi_2O_6$	4,11
α-calcium aluminum fluoride	$CaAlF_5$	5
Anglesite	$PbSO_4$	3
Anhydrite	$CaSO_4$	1,3
Aphthitalite	$(Na,K)_2SO_4$	1,3,4,5,7,10
Aragonite, calcite	$CaCO_3$	3
Avogadrite	KBF_4	3
Bannermanite	$(Na,K)_xV_6O_{15}$	8,9
Bararite	$(NH_4)_2SiF_6$	3
Barite	$BaSO_4$	3
Blossite	α-$Cu_2V_2O_7$	8,9
Cannizorite	Pb,Bi,S	1
Cassiterite	SnO_2	3
Cs-K Sulfate	*	4
Chalcocite	Cu_2S	3
Chalcocyanite	$CuSO_4$	3,4
Chalcopyrite	$CuFeS_2$	1
Chlormanganokalite	K_4MnCl_6	3
Chloromagnesite	$MgCl_2$	3
Contunnite	$PbCl_2$	3
Cu-Fe Sulfide	*	1
Covellite	CuS	3,10
Cristobalite	SiO_2	1,3,4,6,11
Cryptohalite	$(NH_4)_2SiF_6$	3,5
Dufrenoysite	$PbAs_2S_5$	1
Ferberite	$FeWO_4$	6
Ferrucite	$NaBF_4$	3
Fingerite	$Cu_{11}O_2(VO_4)_6$	8,9
Fluorite	CaF_2	3
Galeite	Na_2SO_4•Na(F,Cl)	5
Galena	PbS†	3,4,6,11
Galenobismutite	$PbBiS_4$	3,11
Glauberite	$Na_2Ca(SO_4)_2$	3
Greenockite	CdS	6
Halite	NaCl	1,2,3,4,5,6,7,10,11,13,14
Hematite	Fe_2O_3	3,10
Hercynite	$FeAl_2O_4$	11
Hieratite	K_2SiF_6	2,3,7
Howardevansite	$NaCuFe_2(VO_4)_3$	9
Hydrophilite	$CaCl_2$	3
K-Ca Sulfate	$K_2Ca(SO_4)_2$	4
Langbeinite	$K_2Mg_2(SO_4)_3$	3
Lawrencite	$FeCl_2$	3
Pb-K Chloride	$PbKCl_3$	4
Lyonsite	$Cu_3Fe_4(VO_4)_6$	8,9
Magnetite	Fe_3O_4	1,3,4,6,11,13,14
Marcasite	FeS_2	3
Massicot	PbO	3
Mcbirneyite	$Cu_3(VO_4)_2$	8,9
Meta-thenardite	Na_2SO_4	5
Molybdenite	MoS_2	1,6,11,12,13
Molysite	$FeCl_3$	3
Nanodtite	$CuCl_2$	3
Native Elements	Ag,As,Au,Br,Cu,Fe,I,Pb,S,Sb,Se,Te,Tl	1,7,11,13
Natrikalite	*	10
Orpiment	As_2S_3	3
Palmierite	$K_2Pb(SO_4)_2$	3,4
K-Zn Sulfate	$K_2Zn(SO_4)(Cl)_3$	4
Pyrite	FeS_2	1,3,4,11,13
Pyrrhotite	$Fe_{1-x}S$	3
Quartz	SiO_2	3
Realgar	AsS	3,10
Rhenium Sulfide	ReS_n	14
Salammoniac	NH_4Cl	1,3,5
Sassolite	H_3BO_3	1,3
Scacchite	$MnCl_2$	3
Scherbinaite	V_2O_5	3,8
Se-minerals	*	2
Si-Fe-K minerals	*	2
Na-K-Fe Sulfate	$(Na,K)_2Fe(SO_4,Cl)_2$	4
Sphalerite	ZnS	3,4,11
Stoiberite	$Cu_5V_2O_{10}$	8,9
Sulfohalite	Na_2SO_4•Na(F,Cl)	3
Sylvite	KCl	1,2,3,4,5,6,7,11,13,14
Tenorite	CuO	3,10
Thenardite	Na_2SO_4	1,3,5
Tl-minerals	*	2
Tridymite	SiO_2	3
Wolframite	$FeWO_4$	12
Wollastonite	$CaSiO_3$	4
Ziesite	β-Cu_2VO_7	8,9
Zn Sulfate	$Zn_3(SO_4)(Cl,OH)_4$	4
Unnamed	$Al_2(SO_4)_3$	3
Unnamed	$Fe_2(SO_4)_3$	3
Unnamed	$KAl(SO_4)_3$	3
Unnamed	$NaAl(SO_4)_2$	3
Unnamed	$Na_3Al(SO_4)_3$	3
Unnamed	$NaFe(SO_4)_2$	3
Unnamed	$Na_3Fe(SO_4)_3$	3
Unnamed	$(Na,K)_4CdCl_6$	6

Hydrated mineral phases have not been included because they are unstable on Venus [*Fegley and Trieman*, 1992].

References are 1, *Stoiber and Rose* [1974]; 2, *Quisefit et al.* [1989]; 3, *Toutain et al.* [1990]; 4, *Symonds et al.* [1987]; 5, *Óskarsson* [1981]; 6, *Bernard and Le Guern* [1986]; 7, *Toutain and Meyer* [1989]; 8, *Hughes et al.* [1987]; 9, *Hughes et al.* [1988]; 10, *Angus and Davis* [1976]; 11, *Le Guern and Bernard* [1982]; 12, *Bernard et al.* [1990]; 13, *Quisefit et al.* [1988]; 14, *Khorzhinsky et al.* [1994].

*Mineralogy not identified.

†*Symonds et al.* [1987] report up to 40% Bi in (Pb,Bi)S

Table 2. Elemental Enrichment Factors of Atmospheric Gas and Particulate Samples for Terrestrial Volcanism

Element	Enrichment Factor	Reference
Se	60,000,000	1
Hg	17,000,000	1
Se	6,000,000	3
S	3,400,000	1
Cd	3,000,000	4
Cl	2,500,000	1
Br	2,100,000	4
Se	1,800,000	4
Re	850,000	3
Cl	780,000	4
Bi	490,000	3
Ir	420,000	1
Au	260,000	4
S	240,000	4
Ag	200,000	4
F	190,000	1
Cd	150,000	3
Pb	130,000	4
Sn	130,000	1
Br	120,000	1
Hg	120,000	4
Cd	110,000	1
Cu	90,000	4
Au	76,000	3
Au	40,000	1
Br	33,000	3
Zn	23,000	4
In	21,000	3
As	19,000	1
Pb	17,000	3
In	15,000	1
As	13,000	4
Cs	11,000	4
W	11,000	3
Ag	10,000	1
Mo	8,700	3
Cs	6,600	3
K	5,800	4
Sb	3,800	4
Na	3,400	4
Sn	2,900	3
S	2,400	3
Sb	1,820	2
Mo	1,800	1
Ni	1,800	4
Ag	1,700	3
Br	1,230	2
Cl	1,070	2
Se	1,010	2
Zn	810	3
Cd	760	2
S	750	2
As	695	2
As	680	3
Sb	540	1
Ni	310	1
W	270	1
Cs	260	1
Co	200	4
Rb	200	3
Zn	160	1

References are 1, taken from *Olmez et al.* [1986]; 2, taken from *Lepel et al.* [1978]; 3, taken from *Symonds et al.* [1987];. 4, taken from *Buat-Ménard and Arnold* [1978]. The data from *Olmez et al.* [1986] are the concentrations of elements collected from Kilauea volcano, Hawaii, using a particulate filter held over active vents on Kilauea's east rift in 1983, ratioed to the composition of U.S. Geological Survey standard basalt for Kilauea. The data from *Lepel et al.* [1978] are the concentrations of elements collected from eruption clouds or plumes of Augustine volcano, Alaska, using a particulate filter system, ratioed to the composition of Augustine ash samples collected from the University of Alaska field station approximately 10 km from the crater. The data from *Symonds et al.* [1987] are the concentrations of elements collected from active fumaroles at Merapi volcano, Indonesia, using a silica tube method, ratioed to the assumed magma composition (determined using a partly degassed 1983 lava and also literature values). The data from *Buat-Ménard and Arnold* [1978] are the concentrations of elements collected from active craters and vents at Mount Etna volcano, Italy, by an air filtration method ratioed to average crustal material.

Metal halide vapors and condensates are predicted to be found in or formed from terrestrial basaltic volcanism [*Naughton et al.*, 1974]. Metal halide gases, in fact, have been observed spectroscopically. *Murata* [1960] observed CuCl in volcanic flames during the 1960 eruption of Kilauea, Hawaii. *Tazieff* [1960] also detected CuCl in volcanic flames at Nyiragongo volcano, Zaire. Sulfides may also be formed in volcanic gases through thermochemical equilibrium with halides typified by reactions such as

$$MS(g) + 2HCl(g) = MCl_2(g) + H_2S(g) \quad (1)$$

$$MS(g) + HCl(g) + 0.5H_2(g) = MCl(g) + H_2S(g) \quad (2)$$

which will determine the $MS(g)/MCl_2(g)$ and $MS(g)/MCl(g)$ ratios (M=metal). Terrestrially, high-temperature volcanic gases are found to be in equilibrium at vent temperatures [*Heald et al.*, 1963; *Giggenbach*, 1975; *Gerlach*, 1980a,b; *Gerlach and Graeber*, 1985; *Gerlach and Casadevall*, 1986; *Quisefit et al.*, 1989].

Figure 1 demonstrates that ideal gas thermochemical equilibrium calculations predicting the presence of CuCl in Kilauea volcanic gas agree with the observational evidence of CuCl [*Murata*, 1960]. The figure shows an equilibrium calculation for the reaction

$$CuS(g) + HCl(g) + 0.5H_2(g) = CuCl(g) + H_2S(g) \quad (3)$$

$$\log_{10} K_{eq} = \log_{10}\left(\frac{X_{CuCl}}{X_{CuS}}\right) + \log_{10} X_{H_2S} - \log_{10} X_{HCl} - \tfrac{1}{2}\log_{10} X_{H_2} - \tfrac{1}{2}\log_{10} P_{TOT} \quad (4)$$

where K_{eq} is the equilibrium constant, X_i is the mixing ratio of the ith gas, and P_{TOT} is the total pressure (taken to be 1 bar). *Gerlach and Graeber* [1985] report ~1% (by volume) H_2 for the composition of Kilauea, Hawaii, volcanic gases for both 1917-1918 and 1983 eruptions and we adopt this value. We use thermodynamic data from literature compilations to calculate K_{eq} for reaction (3) [*Mills*, 1974; *Chase et al.*, 1975; *Gurvich et al.*, 1978-1982; *Barin*, 1989; *Knacke et al.*, 1991]. Also shown on Figure 1 are the ranges of H_2S/HCl ratios and equilibrium (vent) temperatures observed for Kilauea by *Gerlach and Graeber* [1985]. Thus, CuCl is predicted to be the dominant Cu-bearing gas for Kilauea volcano. We lack the

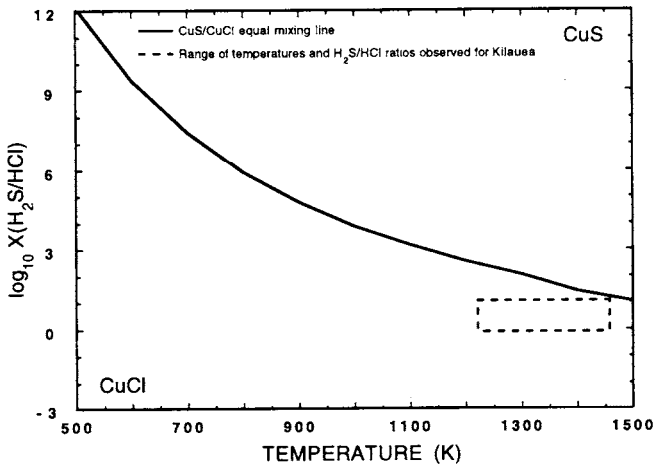

Figure 1. The predicted abundance of CuCl in Kilauea volcanic gases as a function of the H_2S/HCl molar ratio. The solid line shows the equilibrium curve between equal amounts of CuS and CuCl gas for a given vent temperature. The dashed box shows the range of temperatures and H_2S/HCl ratios observed for Kilauea volcanic gas [*Gerlach and Graeber*, 1985].

necessary data to make similar calculations for Nyiragongo volcano, as it is not so well studied as Kilauea.

With some plausible assumptions, it is also possible to determine quantitatively the partitioning of metals between halides and sulfides on Venus, despite our lack of knowledge of Venusian volcanic gas composition. In the case of equation (1), partitioning between metal sulfides and halides will be controlled by the H_2S and HCl abundances, the total pressure, and the temperature at the volcanic vent. In the case of equation (2), partitioning will also be controlled by the H_2 abundance. We know nothing about the mixing ratio of H_2 in volcanic gases on Venus, so we will concentrate on equation (1) which is independent of the mixing ratio of H_2. Figure 2 shows a plot of the mixing ratio of H_2S versus HCl and the phase boundaries along which the metal sulfides and metal chlorides have equal abundances for selected metals at a vent temperature of 1300 K. This vent temperature was selected by analogy with terrestrial volcanic gases which typically equilibrate at temperatures of 1300 K [*Gerlach and Graeber*, 1985]. We use a total pressure of 100 bars (i.e., the mean surface pressure of Venus). Also shown are the observed Venusian atmospheric abundances of 3±2 ppm H_2S [*Hoffman et al.*, 1980a,b] and 0.5 ppm HCl [*Connes et al.*, 1967; *Bézard et al.*, 1990; *Pollack et al.*, 1993]. The plot shows that if an H_2S mixing ratio close to 3 ppm is appropriate, As, Cd, Pb, Sn, and Zn in Venusian volcanic gases will be dominantly in the form of sulfides. However, for significantly lower H_2S mixing ratios of the order of 0.1 ppm, these metals will dominantly be present as chlorides or possibly fluorides.

We have just addressed the thermodynamic stability of metal phases in volcanic gases. Following the eruption of these volcanic phases, three types of reactions may occur. First, the metal phase may exist in equilibrium with Venus surface conditions. Second, the metal phase may react to form another volatile phase. Third, the metal phase may react to form a more refractory phase. In the third case, the volatilities of refractory phases (e.g., metal silicates or oxides) are very low and metals sequestered in refractory phases will be immobile to vapor transport. However, the time scales of vapor transport (as discussed below) are likely to be faster than the time scales of refractory phase formation, as the kinetics of silicate and oxide formation are likely to be slow under Venus surface conditions.

Description of the Vapor Transport Model

Vapor transport is modeled using a one-dimensional box model composed of 100 isothermal 10-km-long pairs of boxes (one atmosphere and one solid), as illustrated in Figure 3. The temperature range is 740 K to 660 K. Mass is transferred between atmosphere boxes through eddy diffusion, governed by Fick's law,

$$\frac{\partial C}{\partial t} = K_{\text{eddy}} \frac{\partial^2 C}{\partial x^2} \tag{5}$$

where C is the concentration of a gas species, t is time, x is lateral distance, and K_{eddy} is eddy diffusivity [*Chapman and Cowling*, 1970; *von Zahn et al.*, 1983]. The meridional eddy diffusivity, K_{eddy}, of the near-surface atmosphere is estimated as 10^8 cm^2 s^{-1} from observed Venera surface wind velocities, u [*McGill et al.*, 1983] (as $K_{\text{eddy}} \sim u\,H$, where H is the scale height), and by analogy with the terrestrial troposphere [*Warneck*, 1988].

Mass is transferred from surface to atmosphere through Langmuir evaporation, which occurs when the partial pressure in a gas reservoir is less than the equilibrium vapor pressure. Evaporation occurs only if solid material is present. From the kinetic theory of gases, the rate of gas molecules striking a surface, for unit mass dm, per unit surface area, dA, per unit time, dt, is

$$\frac{dm}{dA\,dt} = \tfrac{1}{4} \rho_g \bar{c} \tag{6}$$

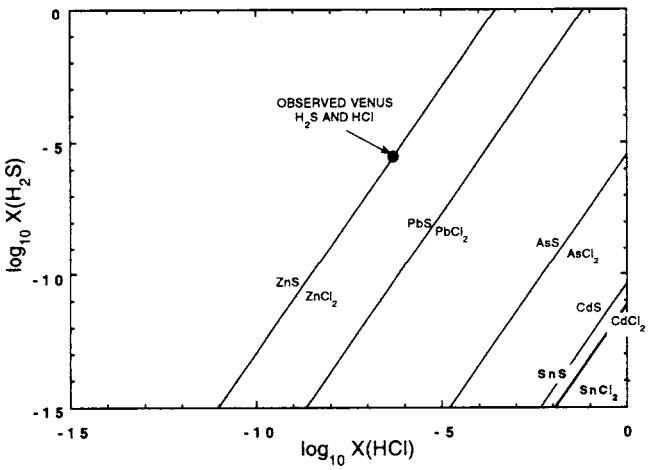

Figure 2. The predicted speciation of metallic vapors in Venusian volcanic gases as a function of the H_2S/HCl molar ratio. The solid lines show phase boundaries along which the metal sulfide and chloride gases have equal abundances. The circle shows the observed H_2S (3±2 ppm) and HCl (0.5±0.2 ppm) abundances in the lower atmosphere of Venus. All calculations are done at a vent temperature of 1300 K and 100 bar total pressure.

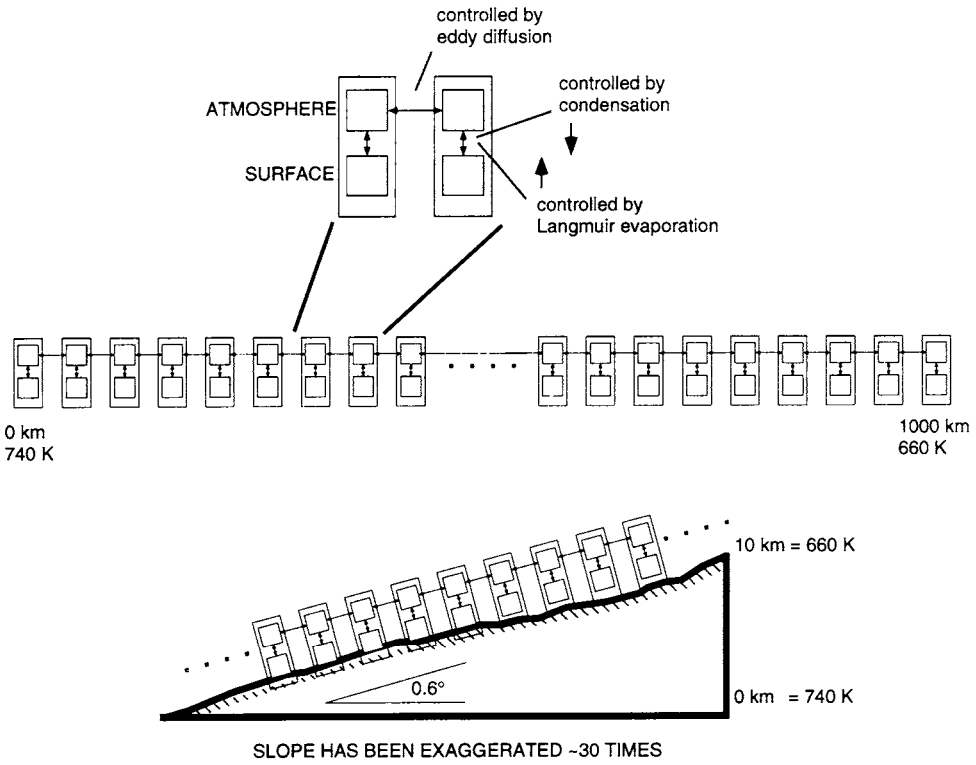

Figure 3. Schematic cartoon showing the one-dimensional finite difference box model.

where ρ_g is the gas density: $\rho_g = P\,M\,/\,R\,T$, where P is partial pressure, M is mean molecular weight, R is the gas constant, and T is temperature. The mean kinetic velocity, $\bar{c}$, is given by $\bar{c} = \sqrt{8\,R\,T\,/\,\pi\,M}$. At equilibrium the pressure exerted by molecules leaving the surface must equal the pressure of molecules striking the surface [*Paule and Margrave*, 1967]. The partial pressure, P, is linearly related to the equilibrium vapor pressure, P_{eq}, by the Langmuir sublimation coefficient, α_L, $P = \alpha_L\,P_{eq}$. The value of α_L lies between >0 and 1, with $\alpha_L = 1$ corresponding to evaporation into a near-vacuum and α_L approaching 0 corresponding to evaporation with large energy or entropy barriers. The value of α_L is near unity if little or no molecular rearrangement occurs during vaporization. This is true for many metal halides and sulfides as the vapor has the same composition as the solid (i.e., congruent vaporization occurs). For all our model conditions, evaporation is more efficient than eddy diffusion and model results are insensitive to any value of $\alpha_L \geq 10^{-3}$. For simplicity, $\alpha_L = 1$ is used in all model runs.

Mass is transferred from atmosphere to surface through condensation. If the partial pressure in a gas reservoir exceeds the equilibrium vapor pressure, mass is condensed until the equilibrium vapor pressure is reached. Mass transfer is solved as a function of time using a finite difference method. The total mass is conserved. Initially, the mass in each gas reservoir is determined from the equilibrium vapor pressure for that reservoir. Each solid box begins with a uniform thickness (i.e., uniform mass).

Model Results

Figure 4 shows results for model runs using high, moderate, and low volatility, $K_{eddy} = 10^8$ cm^2 s^{-1}, and a uniform initial surface layer thickness of 1 cm spread over the entire grid. The thickness of the surface layer is plotted as a function of time versus elevation above mean Venus radius. Transport of several centimeters of material to high elevation occurs over timescales of thousands to millions of years (for high and moderate volatility phases). Little transport occurs for low volatility phases. Three general features are observed. First, the transition from areas with no surface material to areas with enhanced (greater than initial) surface layer thicknesses is abrupt. This is due to two factors: (1) the hottest reservoir with solid material loses material to colder boxes and gains no material, and (2) the average residence time is inversely proportional to T. Second, material accumulates at the coldest reservoir (highest elevation) because of mass balance and down-gradient vapor transport. Third, transport of material to the highlands occurs nonlinearly with respect to time due to the exponential dependence of vapor pressure on T.

For all model runs, the rate of transport from surface to atmospheric boxes is more efficient than the rate of transport between atmospheric boxes. In these cases, the rate of transport is linearly proportional to K_{eddy}. Reducing K_{eddy} by a factor of 10 increases the timescale by a factor of 10. The K_{eddy} used in our model runs is probably an upper limit on the actual Venusian K_{eddy}. Surface roughness, steep slopes, and lower mean wind speeds will lower K_{eddy} [*Rossow*, 1978].

Figure 5 shows the volatility of selected metal halides and chalcogenides compared with the high, medium, and low volatility runs. The ratio of the vapor pressure at 740 K to the vapor pressure at 660 K is plotted against the vapor pressure at 740 K in bars. Small solid symbols correspond to selected metal halides and sulfides whose vapor pressures were determined using thermodynamic data [*Knacke et al.*, 1991]. Also shown are large circles representing model runs. The timescale of transport of a given metal halide or sulfide can be

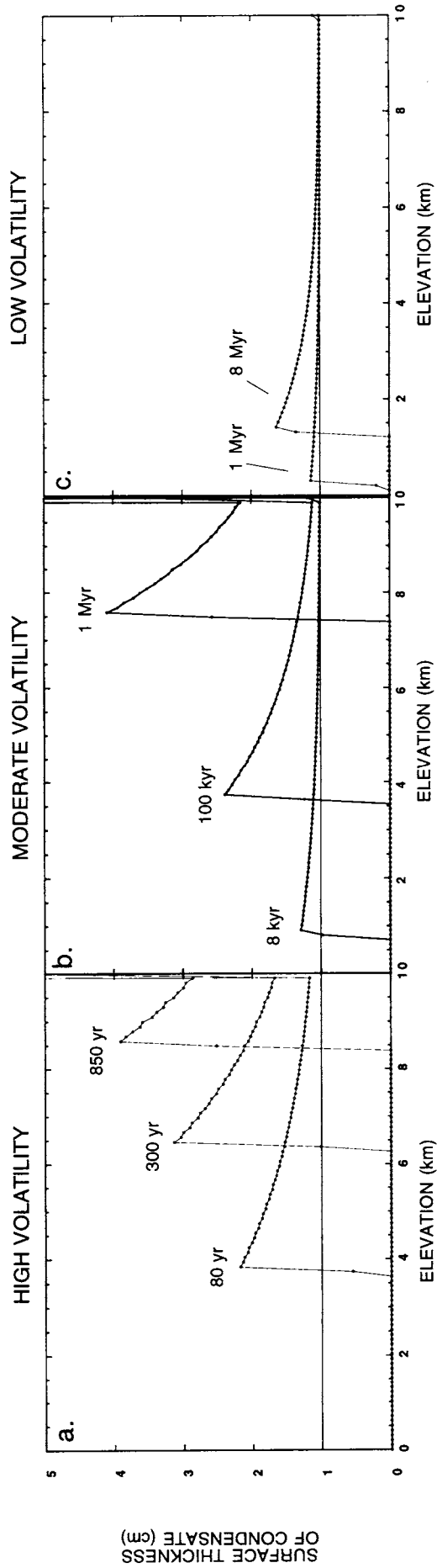

determined by comparing the metal phase with the timescale for the nearest model run. Metal phases with vapor pressures $>10^{-3}$ bar (at 740 K) are transported more quickly than the high volatility model run. Metal phases with vapor pressures $<10^{-10}$ bar (at 740 K) require >10 m.y. for significant transport to occur.

The model described above implicitly assumes that the solid volatiles are in contact with the Venusian atmosphere. As volatiles may be produced in successive volcanic events, it is possible that some material will be buried. This material will be transported more slowly, as its transport is limited by the timescale required for diffusion through the pore space of rocks and soil into the atmosphere. The approximate timescale of diffusion through the solid surface can be estimated from Darcy's law (in one-dimension),

$$u_D = \frac{-k}{\mu}\frac{dp}{dz} \tag{7}$$

where u_D is the volumetric flow rate per unit area (e.g., the Darcy velocity), k is the permeability of the medium, μ is the dynamic viscosity of the fluid, p is pressure, and z is height [*Turcotte and Schubert*, 1982]. The pressure gradient term is $\rho_g\, g\, \Delta h$, where ρ_g is the density of the gas, g is the gravitational acceleration, and Δh is the depth. The dynamic viscosity of an ideal gas can be written $\mu = \frac{1}{3}\rho_g \bar{c} l$, where $\bar{c}$ is the kinetic velocity of the gas and l is the mean free path of the gas ($l = 1/n\, \pi\, d^2$, where n is the number density of gas molecules and d is the diameter of the gas molecule) [*Kittel and Kroemer*, 1980]. Using $k = 10^{-20}$ m^2 (appropriate for impervious rock such as basalt [*Turcotte and Schubert*, 1982]), $\mu = 3 \times 10^{-14}$ Pa s (appropriate for an ideal gas of moderate volatility at 740 K, as in Figure 4b, with a molecular weight of 0.06 kg mol^{-1} and a mean free path of 100 μm), and Venusian gravitational acceleration, the Darcy velocity of a parcel of gas buried at 100-m depth is 10^{-15} m s^{-1}. The actual velocity of the gas will be linearly proportional to the porosity of the solid. Therefore, volatile material buried by associated volcanism will require very long time periods (billions of years) to diffuse through solid rock. We stress, however, that the high enrichment factors (cf. Table 2) of metal halides and chalcogenides are strong evidence that these phases are found in volcanic vapors and aerosols and not trapped beneath solid rock.

Implications for Surface Weathering

Volatile phases may speed mechanical and chemical weathering. Precipitation and growth of salt crystals are observed to disaggregate rocks on the Earth [*Clayton*, 1975; *Colman and Dethier*, 1986]. Salt weathering has also been

Figure 4. Thickness of surface condensate layer versus elevation above the Venus mean as a function of time. (a) High volatility corresponds to a vapor pressure at 740 K of $10^{-3.5}$ bar, and a vapor pressure at 660 K of $10^{-5.2}$ bar. (b) Moderate volatility corresponds to a vapor pressure at 740 K of $10^{-6.7}$ bar, and a vapor pressure at 660 K of $10^{-8.7}$ bar. (c) Low volatility corresponds to a vapor pressure at 740 K of $10^{-9.6}$ bar, and a vapor pressure at 660 K of $10^{-12.2}$ bar.

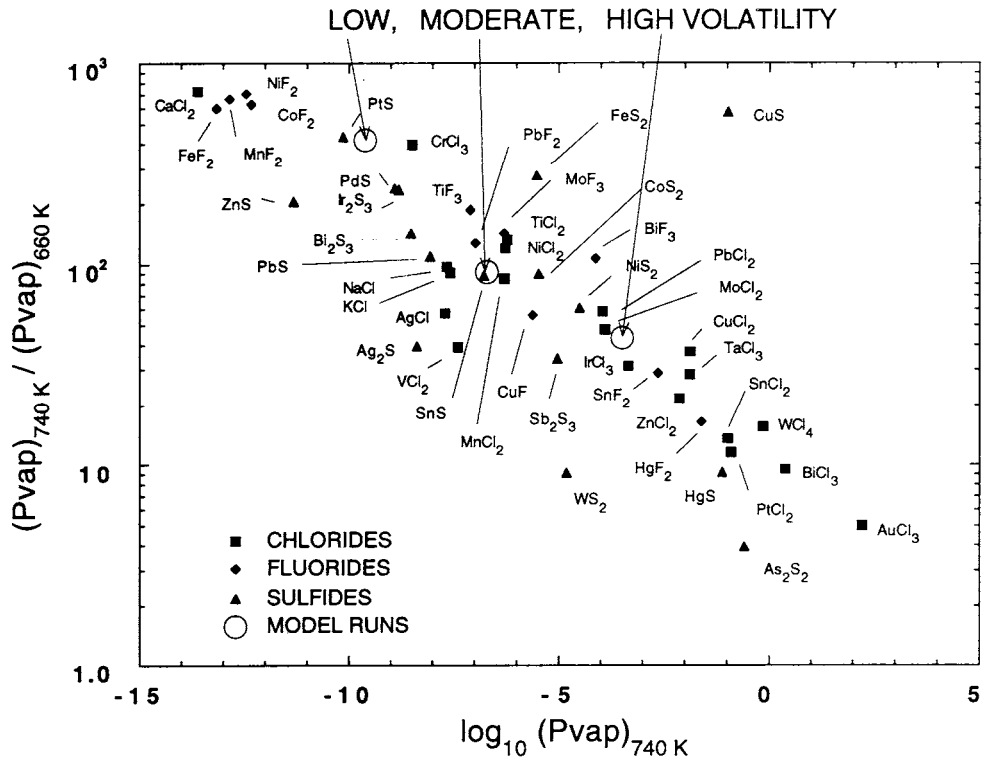

Figure 5. The ratio of the vapor pressure at 740 K to the vapor pressure at 660 K versus the vapor pressure at 740 K in bars. The small solid symbols correspond to selected metal halides and sulfides [*Knacke et al.*, 1991]. The large open circles correspond to model runs.

suggested as an erosive agent on Mars [*Malin*, 1974]. Terrestrially, salt weathering is usually accompanied by the presence of water, but it is important to note that salt weathering can occur simply due to the process of crystal precipitation from a supersaturated fluid and does not explicitly require water. Crystal growth due to the condensation of a supersaturated metal halide or chalcogenide gas can in principle cause salt weathering on Venus.

At equilibrium with a saturated fluid, large crystals grow at the expense of small crystals, minimizing Gibbs free energy [*Wellman and Wilson*, 1965]. Large crystals will exert sufficient pressure to mechanically fracture rock along pores and cracks [*Wellman and Wilson*, 1968]. The necessary conditions for salt weathering on Venus are a supply of salts (i.e., metal halides or chalcogenides) and a temperature at which salts will condense. Equating the work done during crystal growth to the work in extending the surface area,

$$(P_S - P_G)\, dV = \sigma\, dA \tag{8}$$

where P_S is the pressure in the solid, P_G is the pressure in the gas, σ is the interfacial tension between the crystal face and its saturated solution, A is the surface area of the crystal, and V is the volume of the crystal [*Wellman and Wilson*, 1968]. In a porous rock with both large and small pores, crystallization is controlled by the balance between increasing work by growing large crystals in large pores which eventually will exert pressure against the walls of the rock and by growing many small crystals in small pores, which greatly increases the surface area. So, the pressure against the walls of the rock can mechanically fracture the rock while still minimizing the total energy of the system by limiting the total surface area.

On Venus, salt weathering would be more efficient in the highlands because (1) the highlands have the largest abundances of metal halides and chalcogenides (cf. Figure 4) and (2) the residence time of metal halides and chalcogenides as solids in the highlands is the largest (due to the exponential dependence of vapor pressure on temperature). At Labyrinth Wright Valley, Antarctica, salt weathering attacks existing joint systems, producing rubbling on the scale of jointing in the rock (meter scale) and also reduces individual grains [*Selby and Wilson*, 1971]. Individual grains are reduced to sand size and then removed by wind [*Selby and Wilson*, 1971]. In the eastern Saudi Arabian desert, salt weathering produces a zone of very intense weathering, typically at cliff bases and pedestal rocks, and also readily detectable deposition of salt crystals (mainly NaCl, but perhaps also $CaSO_4 \cdot 1/2H_2O$, $Na_2CO_3 \cdot H_2O$, Na_2SO_4, $MgSO_4 \cdot H_2O$, or $CaCl_2$) [*Chapman*, 1980]. A lower limit on the rate of weathering can be derived from the age of the weathered units. In Labyrinth Wright Valley, the observed weathering has occurred since the last advance of the Wright Valley Glacier to the Ross Sea (~2.7 Ma) [*Selby and Wilson*, 1971]. In eastern Saudi Arabia, the weathered bedrock is the Hofuf formation, which is either late Miocene or Pliocene in age (i.e., <11.2 Ma) [*Chapman*, 1980]. Terrestrially, meters of weathering occur over a timescale of tens of millions of years, corresponding to rates of 0.1 $\mu m\ yr^{-1}$.

Thus, by analogy with the Earth, salt weathering may produce a meter-scale rubbled zone of weathering, accompanied by deposition of metal halides and chalcogenides in the highlands over timescales of tens of millions of years. This model is consistent with Very Long Array/Goldstone

radar observations of Venus [*Tryka and Muhleman*, 1992]. If *Tryka and Muhleman* [1992] are correct and the highlands of Venus consist of rocks embedded in a dry low-loss soil layer, salt weathering provides a geologically plausible mechanism for creating such a surface.

Implications for Microwave Emissivity

Vapor transport of metal halides and chalcogenides may play both an active and passive role in weathering on Venus. Metal halides and chalcogenides may actively cause weathering, as discussed above. They will also condense from the atmosphere as layers and passively coat existing rock surfaces. Sufficiently thick condensate layers would be detectable in Magellan emissivity data, if the material had a dielectric constant different from that of the rock being coated. For a two-layer infinite half-space, the microwave emissivity (complement of power reflectivity), e, from the surface is

$$e = 1 - \frac{R_1 + (R_2 / L^2)(1 - 2R_1)}{[1 - (R_1 R_2 / L^2)]} \quad (9)$$

where $R_1 = R_1(\theta,\varepsilon)$ and $R_2 = R_2(\theta,\varepsilon)$ are the directional power reflectivities (from Fresnel's laws for complex dielectric constants) of the first and second layer, respectively, $L = L(\theta,\varepsilon,\lambda,d)$ is the loss factor in the first layer (plate), θ is the emission angle, λ is the radar wavelength in the first layer, and d is the thickness of the first layer [*Ulaby et al.*, 1982] (see Figure 6 for the geometry of the model). The model employs geometric scattering and thus it is assumed that $d \geq \lambda$. Volume scattering is ignored, and the Rayleigh-Jeans approximation is used. Finally, the emission is assumed to be incoherent in phase (e.g., $d \neq n\lambda$, where n is an integer) For selected metal halides and chalcogenides, thin (≤few centimeters) layers have sufficiently high dielectric constants to match the observed highland emissivities. Table 3 lists metal halides and chalcogenides with dielectric constants greater than 10.

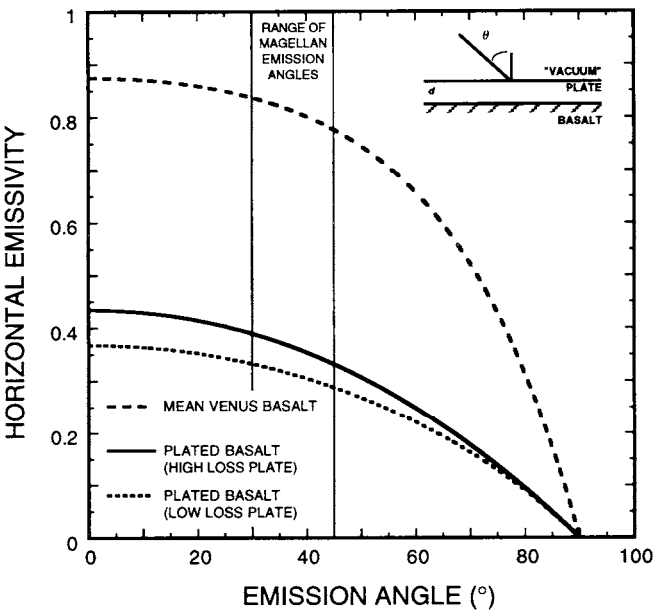

Figure 6. Plot of horizontally polarized emissivity versus emission angle for the mean Venus dielectric constant of ~4.4 (e.g., basalt surface) [*Pettengill et al.*, 1992], for a basalt surface coated with a low-loss layer with a real dielectric constant of 49, and for a basalt surface coated with a high-loss layer with a real dielectric constant of 49. Inset in upper right shows schematic cartoon of the plate model. Also shown is the range of emission angles observed by Magellan during the first cycle of data collection.

Table 3. Dielectric Constants of Selected Halides and Chalcogenides

Mineral Formula	Dielectric Constant ε
WO_3	6,000–90,000*
SbSI	2,000–50,000*
PbTe	400
PbSe	280
PbO†	200
PbS†	190
Sb_2S_3†	180
Sb_2Se_3	110
$PbCl_2$†	34
TlCl	32
PbF_2	26
HgCl	14
AgCl	11
LiCl	11
CuCl‡	10
$BaCl_2$	10

Dielectric constants measured at radar wavelengths; data taken from *Young and Frederikse* [1973].

*These phases are ferroelectric [*Lines and Glass*, 1977]. Other ferroelectric phases include GeTe and $CsGeCl_3$ [*Lines and Glass*, 1977].

†This mineral has been detected as a terrestrial volcanic sublimate (see Table 1).

‡CuCl gas has been detected spectroscopically at both Kilauea [*Murata*, 1960] and Nyiragongo [*Tazieff*, 1960].

Figure 6 shows a plot of horizontally linearly polarized emissivity versus emission angle for average Venus basalt, for average Venus basalt coated with a high-loss layer and having a real dielectric constant of 49, and for average Venus basalt coated with a low-loss layer and having a real dielectric constant of 49. At emission angles typically observed by the Magellan Synthetic Aperture Radar antenna (30°–45°) [Pettengill *et al.*, 1992], observed Venus highland emissivities correspond to both the high-loss and low-loss model emissivities. The low-loss model emissivity has lower emissivity than the high-loss model, as multiple reflections raise the reflectivity and thus lower the emissivity. Note that the plate model does not incorporate textural effects; it assumes a flat half-space. Surfaces which are rougher than a half-space will have higher horizontally polarized emissivities and lower vertically polarized emissivities for a given dielectric constant [*Ulaby et al.*, 1982].

Tryka and Muhleman [1992] report that observations of a highland region (Alpha Regio) using Earth-based VLA/Goldstone radar show strong depolarized reflectivities at high elevations and normal depolarized reflectivities in the lowlands. They attribute the strong depolarized reflectivities to scattering from a surface consisting of common Venusian rocks embedded in a dry soil layer. Two other mechanisms can

explain these observations: (1) young, rough, terrestrial volcanic surfaces have depolarized reflectivities as high as those observed in Alpha Regio [*Campbell and Campbell*, 1992], and (2) multiple reflections from a moderately rough high-dielectric plate or surface would account for the strong depolarized reflectivities [*Campbell et al.*, 1993]. Thus, the observed strongly depolarized reflectivities do not preclude either a plating model (i.e., surface scattering) or a weathered zone model (i.e., volume scattering).

The Magellan mission also collected vertical linear polarization emissivity over lowland and highland regions. The observed vertical and horizontal emissivity over smooth lowland areas are wholly consistent with surface scattering being responsible for observed microwave signatures [*Arvidson et al.*, 1994]. *Arvidson et al.* [1994] show that surface scattering (consistent with a surface plated by metal halides and chalcogenides) dominates the highlands radar scattering signature of Ovda Regio; however, ratios of vertical to horizontal radar specific cross section in the highlands exceed unity in places and seem to be correlated with geology, suggesting volume scattering (consistent with a highly weathered soil layer) may occur in regions.

Implications for Hazes in the Near-Surface Atmosphere of Venus

Ragent and Blamont [1980] found statistically significant increases in the backscatter cross-section recorded by the Pioneer Venus Nephelometer Experiment between altitudes of 5.8 and 6.4 km. Both the Pioneer Venus night probe and Pioneer Venus north probe detected increases in backscatter cross section. This increase may be due to the presence of low-altitude metal halide or chalcogenide hazes. The Pioneer Venus cloud particle spectrometer (LCPS) experiment failed to detect any aerosol particles below 31 km [*Knollenberg and Hunten*, 1980]. However, noise bursts in the lower few kilometers of the atmosphere may have masked evidence of actual particles, and therefore the possibility of particles not detected by LCPS in the lower atmosphere exists [*Knollenberg and Hunten*, 1980]. *Knollenberg and Hunten* [1980] state, however, that no particles >2 μm in size were detected. Thus, a low-altitude haze would have to consist of particles <2 μm in size. For comparison, the mean diameters of particles in the other cloud layers on Venus are 0.4 μm (upper haze), 0.4 μm (upper cloud), 0.3 μm (middle cloud), 0.4 μm (lower cloud), 0.2 μm (lower haze), and 0.3 μm (precloud layers) [*Knollenberg and Hunten*, 1980]. So, the upper limit of 2 μm does little to preclude the possibility of a near-surface haze. Unfortunately, the lack of particle size data at low elevations means that the inversion of Pioneer Venus nephelometer data to obtain indices of refraction and particle sizes is not unique. In conclusion, the presence of a near-surface haze (of metal halides or chalcogenides?) is supported by the Pioneer Venus Nephelometer Experiment and not rejected by the Pioneer Venus cloud particle spectrometer experiment.

All instruments aboard Pioneer Venus entry probes having external sensors failed at an altitude of 12.5 km [*Colin*, 1980]. Preflight and postflight testing revealed no material or design deficiencies. Furthermore, the combined effects of sulfuric acid, pressure, and temperature were not responsible for the failures [*Colin*, 1980]. *Polaski* [1993] suggests that the anomalies are related to ion accumulation on the probe surface, caused perhaps by a charged layer in the lower atmosphere or perhaps by chemical reactions on probe external surfaces. *Fegley* [1993] suggests that the 12.5-km anomaly may have been caused by condensation of conductive metal species from volcanic vents (e.g., metal halides or chalcogenides) onto the Pioneer Venus probes. These conductive species would provide a cause for ion accumulation. In conclusion, the Pioneer Venus 12.5-km anomaly may have been the result of metal halides or chalcogenides in the near-surface atmosphere of Venus.

Conclusion

We have demonstrated that the volatile transport of significant quantities of moderately to highly volatile metal halides and chalcogenides (as well as other volatile phases) from the hot lowlands to the cold highlands of Venus at rates of 0.01 to >10 μm yr^{-1} occurs. Volcanic emissions on Venus, by analogy with those on the Earth, provide a significant source of metal halides and chalcogenides. Diffusive migration over timescales of ~1–10 m.y. can result in the accumulation of millimeters to centimeters of metal halides and chalcogenides. Some metal halides and chalcogenides have high dielectric constants, and the plating of these phases would be observable by Magellan, for sufficiently thick plates. In addition to plating on the surface, growth of metal halide and chalcogenide crystals could weather highland surfaces, akin to salt weathering on the Earth, which can weather meters of material over a timescale of 10 m.y. Further analyses of microwave backscatter and emissivity data should be able to determine which scattering model is more plausible: high dielectric plate (dominated by surface scattering) or low-loss soil layer (dominated by volume scattering). Finally, the presence of volatile phases at high altitudes on Venus may be responsible for low-altitude (6 km elevation) hazes observed by Pioneer Venus and also for low-altitude (12.5 km elevation) failure of external sensors on the Pioneer Venus probes.

Finally, the presence of volatile metal halide and chalcogenide vapors in the near-surface atmosphere of Venus is testable by Earth-based spectral observations in several infrared regions which penetrate down to the surface of Venus [*Crisp et al.*, 1989; *Pollack et al.*, 1993]. Direct evidence of the role of vapor transport of metal halides and chalcogenides could also be provided by a lander at high elevation (>6054 km) on Venus capable of elemental analysis (e.g., XRF or α-particle backscatter) or mineralogical identification (e.g., X ray diffraction or scanning electron microscopy). The necessary instruments have either been flown on past spacecraft missions or developed for proposed missions.

Acknowledgments. B.F. is supported by grants NAGW-2867 and NAGW-3446 from the NASA VDAP and Planetary Atmospheres Programs. R.E.A. is supported by NASA Planetary Geology and Geophysics Program Grant NAGW-1358. A review by Lionel Wilson improved the text.

References

Andreichikov, B.M., I.K. Akhmetshin, B.N. Korchuganov, L.M. Mukhin, B.I. Ogorodnikov, I.V. Petryanov, and V.I. Skitovich, X-ray

radiometric analysis of Venus cloud aerosols by Vega-1 and -2 automated interplanetary probes, *Cosmic Res., 25,* 554-567, 1987.

Angus, J.G., and G.R. Davis, Base metal enrichment in volcanic sublimates and secondary alteration products from Vesuvius and Vulcano, *Min. Mag., 40,* 481-486, 1976.

Arvidson, R.E., R.A. Brackett, M.K. Shepard, N.R. Izenberg, B. Fegley Jr., and J.J. Plaut, Microwave signatures and surface properties of Ovda Regio and surroundings, Venus, *Icarus,* in press, 1994.

Barin, I., ***Thermochemical Data of Pure Substances,*** vols I and II, VCH Weinheim, Germany, 1989.

Barsukov, V.L., I.L. Khodakovsky, V.P. Volkov, Yu.I. Sidorov, V.A. Dorofeeva, and N.E. Andreeva, Metal chloride and elemental sulfur condensates in the Venusian troposphere: Are they possible?, *Proc. Lunar Planet. Sci. Conf., 12th,* 1517-1532, 1981.

Bernard, A., and F.L. Le Guern, Condensation of volatile elements in high-temperature gases of Mount St. Helens, *J. Volcanol. Geotherm. Res., 28,* 91-105, 1986.

Bernard, A., R.B. Symonds, and W.I. Rose Jr., Volatile transport and deposition of Mo, W, and Re in high temperature magmatic fluids, *Appl. Geochem., 5,* 317-326, 1990.

Bézard, B., C. deBergh, D. Crisp, and J.P. Maillard, The deep atmosphere of Venus revealed by high-resolution nightside spectra, *Nature, 345,* 508-511, 1990.

Buat-Ménard, P., and M. Arnold, The heavy metal chemistry of atmospheric particulate matter emitted by Mount Etna Volcano, *Geophys. Res. Lett., 5,* 245-248, 1978.

Campbell, B.A., and D.B. Campbell, Analysis of volcanic surface morphology on Venus from comparison of Arecibo, Magellan, and terrestrial airborne radar data, *J. Geophys. Res., 97,* 16,293-16,314, 1992.

Campbell, B.A., R.E. Arvidson, and M.K. Shepard, Radar polarization properties of volcanic and playa surfaces: Applications to terrestrial remote sensing and Venus data interpretation, *J. Geophys. Res., 98,* 17,099-17,114, 1993.

Chapman, R.W., Salt weathering by sodium chloride in the Saudi Arabian desert, *Am. J. Sci., 280,* 116-129, 1980.

Chapman, S., and T.G. Cowling, ***The Mathematical Theory of Non-Uniform Gases,*** 423 pp., Cambridge University Press, New York, 1970.

Chase, W.M., *et al.* (Eds.), JANAF thermochemical tables, 3rd ed., *J. Phys. Chem. Ref. Data 14,* suppl. 1, 1975.

Clayton, K.M., ***Weathering***, 304 pp., Longman, New York, 1975.

Colin, L., The Pioneer Venus Program, *J. Geophys. Res., 85,* 7575-7598, 1980.

Colman, S.M., and D.P. Dethier, ***Rates of Chemical Weathering of Rocks and Minerals,*** 603 pp., Academic, San Diego, Calif., 1986.

Connes, P., J. Connes, W.S. Benedict, and L.D. Kaplan, Traces of HCl and HF in the atmosphere of Venus, *Astrophys. J., 152,* 731-743, 1967.

Crisp, D., W.M. Sinton, K.W. Hodapp, B. Ragent, F. Gerbault, J.H. Goebel, R.G. Probst, D.A. Allen, K. Pierce, and K.R. Stapelfeldt, The nature of the near-infrared features on the Venus night side, *Science, 246,* 506-509, 1989.

Fegley, B. Jr., Comments on chemical scenarios, paper presented at Pioneer Venus Probe 12.5 km anomaly workshop, NASA Ames Research Center, Moffett Field, CA, 1993.

Fegley, B., Jr., and A.H. Treiman, Chemistry of atmosphere-surface interactions on Venus and Mars, in ***Venus and Mars: Atmospheres, Ionospheres, and Solar Wind Interactions,*** *Geophys. Monogr.*, vol. 66, edited by J. Luhmann et al., pp. 7-71, AGU, Washington, D.C., 1992.

Fegley, B., Jr., A.H. Treiman, and V.L. Sharpton, Venus surface mineralogy: Observational and theoretical constraints, *Proc. Lunar Planet. Sci. Conf., 22nd,* 3-19, 1992.

Fegley, B., Jr., K. Lodders, and G. Klingelhöfer, Kinetics and mechanism of pyrite decomposition on the surface of Venus, *Bull. Am. Astron. Soc., 25,* 1094, 1993.

Gerlach, T.M., Evaluation of volcanic gas analyses from Kilauea volcano, *J. Volcanol. Geotherm. Res., 7,* 295-317, 1980a.

Gerlach, T.M., Investigation of volcanic gas analyses and magma outgassing from Erta' Ale lava lake, Afar, Ethiopia, *J. Volcanol. Geotherm. Res., 7,* 415-441, 1980b.

Gerlach, T.M., and T.J. Casadevall, Evaluation of gas data from high-temperature fumaroles at Mount St. Helens, 1980–1982, *J. Volcanol. Geotherm. Res., 28,* 107-140, 1986.

Gerlach, T.M., and E.J. Graeber, Volatile budget of Kilauea volcano, *Nature, 313,* 273-277, 1985.

Giggenbach, W.F., A simple method for the collection and analysis of volcanic gas samples, *Bull. Volcanol., 39,* 132-145, 1975.

Gurvich, L.V., et al., ***Termodinamicheskie sovoistava indinvidual'nykh veshshestv,*** vols. 1-4, High Temperature Institute, Moscow, Russia, 1978-1982.

Heald, E.F., J.J. Naughton, and I.L. Barnes Jr., The chemistry of volcanic gases, 2., Use of equilibrium calculations in the interpretation of volcanic gas samples, *J. Geophys. Res., 68,* 545-557, 1963.

Hoffman, J.H., V.I. Oyama, T.M. Donahue, and M.B. McElroy, Composition of the Venus lower atmosphere from the Pioneer Venus mass spectrometer, *J. Geophys. Res., 85,* 7882-7890, 1980a.

Hoffman, J.H., V.I. Oyama, and U. von Zahn, Measurements of the Venus lower atmosphere composition: A comparison of results, *J. Geophys. Res., 85,* 7871-7881, 1980b.

Hughes, J.M., S.J. Starkey, M.L. Malinconico, and L.L. Malinconico, Lysonite, $Cu_3^{2+}Fe_4^{3+}(VO_4)_6^{3-}$, a new fumarolic sublimate from Izalco volcano, El Salvador: Descriptive mineralogy and crystal structure, *Am. Mineral., 72,* 1000-1005, 1987.

Hughes, J.M., J.W. Drexler, C.F. Campana, and M.L. Malinconico, Howardevansite, $NaCu^{2+}Fe_2^{3+}(VO_4)_3^{3-}$, a new fumarolic sublimate from Izalco volcano, El Salvador: Descriptive mineralogy and crystal structure, *Am. Mineral., 73,* 181-186, 1988.

Khorzhinsky, M.A., S.I. Tkachenko, K.I. Shmulovich, Y.A. Taran, and G.S. Steinberg, Discovery of a pure rhenium mineral at Kudriavy volcano, *Nature, 369,* 51-52, 1994.

Kittel, C., and H. Kroemer, ***Thermal Physics,*** 473 pp., W.H. Freeman, New York, 1980.

Klingelhöfer, G., B. Fegley Jr., and K. Lodders, ^{57}Fe Mössbauer studies of the kinetics of pyrite decomposition on the surface of Venus (abstract), *Lunar Planet. Sci., XXV,* 707-708, 1994.

Knacke O., O. Kubaschewski, and K. Hesselmann, ***Thermochemical Properties of Inorganic Substances,*** vols I and II, Springer-Verlag, Berlin, 1991.

Knollenberg, R.G., and D.M. Hunten, The microphysics of the clouds of Venus: Results of the Pioneer Venus Particle Size Spectrometer Experiment, *J. Geophys. Res., 85,* 8039-8058, 1980.

Kuz'min, A.D., Radio astronomical studies of Venus, in ***Venus,*** edited by D.M. Hunten, L. Colin, T.M. Donahue, and V.I. Moroz, pp. 36-44, University of Arizona Press, Tucson, 1983.

Le Guern, F., and A. Bernard, A new method for sampling and analyzing volcanic sublimates–Application to Merapi Volcano, Java, *J. Volcanol. Geotherm. Res., 12,* 133-146, 1982.

Lepel, E.A., K.M. Stefansson, and W.H. Zoller, The enrichment of volatile elements in the atmosphere by volcanic activity: Augustine Volcano 1976, *J. Geophys. Res., 83,* 6213-6220, 1978.

Lewis, J.S., An estimate of the surface conditions of Venus, *Icarus, 8,* 434-456, 1968.

Lewis, J.S., Geochemistry of the volatile elements on Venus, *Icarus, 11,* 367-385, 1969.

Lewis, J.S., and B. Fegley Jr., Venus: Halide cloud condensation and volatile element inventories, *Science, 216,* 1223-1225, 1982.

Lines, M.E., and A.M. Glass, ***Principles and Applications of Ferroeclectrics and Related Materials,*** 680 pp., Clarendon Press, Oxford, 1977.

Malin, M.C., Salt weathering on Mars, *J. Geophys. Res., 79,* 3888-3894, 1974.

McGill, G.E., J.L. Warner, M.C. Malin, R.E. Arvidson, E. Eliason, S. Nozette, and R.D. Reasenberg, Topography, surface properties, and tectonic evolution, in ***Venus,*** edited by D.M. Hunten, L. Colin, T.M.

Donahue, and V.I. Moroz, pp. 69-130, University of Arizona Press, Tucson, 1983.

Mills, K.C., *Thermodynamic Data for Inorganic Sulphides, Selenides, and Tellurides*, 845 pp., Butterworths, London, 1974.

Murata, K.J., Occurrence of CuCl emission in volcanic flames, *Am. J. Sci., 258*, 769-772, 1960.

Naughton, J.J., V.A. Lewis, D. Hammond, and D. Nishimoto, The chemistry of sublimates collected directly from lava fountains at Kilauea Volcano, Hawaii, *Geochim. Cosmochim. Acta, 38*, 1679-1690, 1974.

Olmez, I., D.L. Finnegan, and W.H. Zoller, Iridium emissions from Kilauea volcano, *J. Geophys. Res., 91*, 653-663, 1986.

Óskarsson, N., The chemistry of icelandic lava incrustations and the latest stages of degassing, *J. Volcanol. Geotherm. Res., 10*, 93-111, 1981.

Paule, R.C., and J.L. Margrave, Free-evaporation and effusion techniques, in *The Characterization of High Temperature Vapors*, edited by J.L. Margrave, pp. 130-151, John Wiley, New York, 1967.

Petryanov, I.V., B.M. Andreychikov, B.N. Korchuganov, E.I. Ovsyankin, B.I. Ogorodnikov, V.I. Skitovich, and V.K. Khristianov, Iron in the Venus clouds, *Dokl. Akad. Nauk SSSR, 260*, 834, 1981.

Pettengill, G.H., and P.G. Ford, Origins of the low values of radiothermal emissivity seen in some parts of Venus, *Eos Trans. AGU, 74*, 189, 1993.

Pettengill, G.H., P.G. Ford, and S. Nozette, Venus: Global surface radar reflectivity, *Science, 217*, 640-642, 1982.

Pettengill, G.H., P.G. Ford, and B.D. Chapman, Venus: Surface electromagnetic properties, *J. Geophys. Res., 93*, 14,881-14,892, 1988.

Pettengill, G.H., P.G. Ford, and R.J. Wilt, Venus surface radiothermal emission as observed by Magellan, *J. Geophys. Res., 97*, 13,091-13,102, 1992.

Polaski, L., Overview of observed anomalies, paper presented at Pioneer Venus Probe 12.5 km anomaly workshop, NASA Ames Research Center, Moffett Field, CA, 1993.

Pollack, J.B., et al., Near-infrared light from Venus' nightside: A spectroscopic analysis, *Icarus, 103*, 1-42, 1993.

Quisefit, J.P., J.P. Toutain, and G. Mouvier, On a thermodynamical model adopted for the condensation of gaseous volcanic emissions (abstract), *Chem. Geol., 70*, 155, 1988.

Quisefit, J.P., J.P. Toutain, G. Bergametti, M. Javoy, B. Cheynet, and A. Person, Evolution versus cooling of gaseous volcanic emissions from Momotombo Volcano, Nicaragua: Thermochemical model and observations, *Geochim. Cosmochim. Acta, 53*, 2591-2608, 1989.

Ragent, B., and J. Blamont, The structure of the clouds of Venus: Results of the Pioneer Venus Nephelometer Experiment, *J. Geophys. Res., 85*, 8089-8105, 1980.

Rossow, W.B., Cloud microphysics: Analysis of the clouds of Earth, Venus, Mars, and Jupiter, *Icarus, 36*, 1-50, 1978.

Seiff, A., Thermal structure of the atmosphere of Venus, in *Venus*, edited by D.M. Hunten, L. Colin, T.M. Donahue, and V.I. Moroz, pp. 215-279, University of Arizona Press, Tucson, 1983.

Selby, M.J., and A.T. Wilson, The origin of the Labyrinth Wright Valley, Antarctica, *Geol. Soc. Am. Bull. 82*, 471-476, 1971.

Shepard, M.K., R.E. Arvidson, R.A. Brackett, and B. Fegley Jr., A ferroelectric model for the highlands of Venus, *Geophys. Res. Lett., 21*, 469-472, 1994.

Stoiber, R.E., and W.I. Rose Jr., Fumarole incrustations at active Central American volcanoes, *Geochim. Cosmochim. Acta, 38*, 495-516, 1974.

Surkov, Yu.A., F.F. Kirnozov, V.I. Guryanov, V.N. Glasov, V. Dunchenko, K. Kurochkin, E. Raspontny, L. Kharitnova, L. Tatsiy, and V. Gimadov, Venus cloud aerosol investigation on the Venera 12 space probe (preliminary data), *Geokhimiya, 18*, 3-9, 1981.

Surkov, Yu.A., et al., Determination of the chemical composition of Venus cloud aerosol on the Vega-1 automated interplanetary probe by the malachite mass-spectrometer, *Cosmic Res., 25*, 574-580, 1987.

Surkov, Yu.A., F.F. Kirnozov, V.N. Glasov, A.G. Dunchenko, and V.V. Astrashkevich, New data on the Venus cloud aerosol (preliminary results of measurements by the Venera 14 probe), *Pis'ma Astron. Zh., 8*, 700, 1982.

Symonds, R.B., W.I. Rose, M.H. Reed, F.E. Lichte, and D.L. Finnegan, Volatilization, transport and sublimation of metallic and non-metallic elements in high temperature gases at Merapi Volcano, Indonesia, *Geochim. Cosmochim. Acta, 51*, 2083-2101, 1987.

Tazieff, H., Exploration geophysique et geochimique du volcan Niragongo (Congo belge), *Bull. Volcanol., 23*, 69-71, 1960.

Toutain, J.P., and G. Meyer, Iridium-bearing sublimates at a hot-spot volcano (Piton de la Fournaise, Indian Ocean), *Geophys. Res. Lett., 16*, 1391-1394, 1989.

Toutain, J.P., P. Aloupogiannis, H. Delorme, A. Person, P. Blanc, and G. Robaye, Vapor deposition of trace elements from degassed basaltic lava, Piton de la Fournaise volcano, Reunion Island, *J. Volcanol. Geotherm. Res., 40*, 257-268, 1990.

Tryka, K.A., and D.O. Muhleman, Reflection and emission properties of Venus: Alpha Regio, *J. Geophys. Res., 97*, 13,379-13,394, 1992.

Turcotte, D.L., and G. Schubert, *Geodynamics: Applications of Continuum Physics to Geological Problems*, 450 pp., John Wiley, New York, 1982.

Ulaby, F.T., R.K. Moore, and A.K. Fung, *Microwave Remote Sensing: Active and Passive*, 3 vols., Addison Wesley, Reading, Mass, 1982.

von Zahn, U., S. Kumer, H. Niemann, and R. Prinn, Composition of the atmosphere, in *Venus*, edited by D.M. Hunten, L. Colin, T.M. Donahue, and V.I. Moroz, pp. 299-430, University of Arizona, Tucson, 1983.

Warneck P., *Chemistry of the Natural Atmosphere, Int. Geophys. Ser.*, vol. 41, 757 pp., Academic, San Diego, Calif., 1988.

Wellman, H.W., and A.T. Wilson, Salt weathering, a neglected geological erosive agent in coastal arid environments, *Nature, 205*, 1097-1098, 1965.

Wellman, H.W., and A.T. Wilson, Salt weathering or fretting, in *Encyclopedia of Geomorphology*, edited by R.W. Fairbridge, Reinhold, New York, 1968.

Young K.F., and H.P.R., Frederikse, Compilation of the Static Dielectric Constant of Inorganic Solids, *J. Phys. Chem. Ref. Data, 2*, 313, 1973.

R. E. Arvidson, R. A. Brackett, and B. Fegley Jr., Department of Earth and Planetary Sciences, Campus Box 1169, Washington University, One Brookings Drive, St. Louis, MO 63130-4899. (e-mail: arvidson@wunder.wustl.edu; brackett@wunder.wustl.edu; bfegley@planet.win.net)

(Received March 28, 1994; revised October 13, 1994; accepted October 13, 1994.)